Diagnostic imaging of osteoporosis and sarcopenia: a narrative review

Carmelo Messina¹, Gabriele Maffi², Jacopo Antonino Vitale³, Fabio Massimo Ulivieri⁴, Giuseppe Guglielmi⁵, Luca Maria Sconfienza²,⁶

¹Unità Operativa di Radiologia Diagnostica ed Interventistica, IRCCS Istituto Ortopedico Galeazzi, Milan, Italy; ²Scuola di Specializzazione in Radiodiagnostica, Università degli Studi di Milano, Milan, Italy; ³IRCCS Istituto Ortopedico Galeazzi, Milan, Italy; ⁴Bone Metabolic Unit, Fondazione IRCCS Ca'Granda Ospedale Maggiore Policlinico, Medicina Nucleare, Milan, Italy; ⁵Radiology Department, University of Foggia, Foggia, Italy; ⁶Dipartimento di Scienze Biomediche per la Salute, Università degli Studi di Milano, Milan, Italy

Correspondence to: Carmelo Messina. Unità Operativa di Radiologia Diagnostica ed Interventistica, IRCCS Istituto Ortopedico Galeazzi, Via Riccardo Galeazzi 4, 20161 Milan, Italy. Email: carmelomessina.md@gmail.com.

Abstract: Osteoporosis and sarcopenia represent two major health problems with an increasing prevalence in the elderly population. The correlation between these diseases has been widely reported, leading to the development of the term "osteosarcopenia" to diagnose those patients suffering from both diseases. Several imaging methods for the diagnosis and management of osteoporosis exist, with dual-energy X-ray absorptiometry (DXA) being the most commonly used for measuring bone mineral density (BMD). Imaging technique other than DXA is represented by conventional radiography, computed tomography (CT) and ultrasound (US). Similarly, the imaging technologies used to detect loss of skeletal muscle mass in sarcopenia include DXA, CT, US and magnetic resonance imaging (MRI). These methods differ in terms of reliability, radiation exposure and costs. CT and MRI represent the gold standard for evaluating body composition (BC), but are costly and time-consuming. DXA remains the most often used technology for studying BC, being quick, widely available and with low radiation exposure.

Keywords: Osteoporosis; sarcopenia; imaging; dual energy X-ray absorptiometry (DXA)

Introduction

Osteoporosis and sarcopenia represent two chronic conditions which prevalence is increasing in the elderly population, both being recognized as a major health problem (1,2). Osteoporosis is defined as a systemic skeletal disease characterized by low bone mass and microarchitectural deterioration of bone tissue, both condition leading to an increase in bone fragility and fracture susceptibility (3). Sarcopenia is a disease characterized by a progressive and global loss of muscle mass and muscle function with advancing age, which leads to a non-negligible impact on daily life activities (2,4). The prevalence of both disease increases with age and is associated with a significant reduction in physical ability. The prevalence of sarcopenia may vary according to its definition, but has been reported around 13% in individuals between 60 and 70 years, despite it can reach reaches almost 50% of people over 80 years of age (4,5). For what concerns osteoporosis, its clinical significance relies on the fractures that may occur, which represent an important cause of morbidity. This is particularly true for hip fractures, as they cause functional impairment, typically leading to hospitalization, and are associated to higher mortality: almost half of osteoporotic-deaths are due to hip fractures (1,6).

The correlation between low bone mineral density (BMD) and muscle weakness has been reported by several studies (7-9). As a consequence, the term "osteosarcopenia"

has been recently introduced to diagnose those patients suffering from both diseases (5). The purpose of this review is to discuss the main quantitative imaging technique currently available to diagnose osteoporosis or sarcopenia, with a special focus on dual-energy X-ray absorptiometry (DXA).

Imaging of osteoporosis

Osteoporosis is still most frequently diagnosed with conventional radiography, with the main radiographic features of systemic osteoporosis being increased radiolucency and cortical thinning (10). Nevertheless, this technique is relatively subjective and has low specificity, as radiological signs can be depicted in advanced stages, when already a significant amount of bone is loss (around 30%) (10). It is therefore mandatory to evaluate bone in early stages of the disease, with densitometric techniques being capable to evaluate even subtle variation in BMD. In fact, among the different factors that influence bone strength, BMD is the one that contributes for approximately 70% and can be easily quantified in clinical practice. The purpose of measure BMD is not only related to diagnose osteoporosis but also to assess fracture risk probability and to monitor patients under pharmacological treatment (11). BMD is the amount of bone mass and can be expressed as areal density (bone mass per unit area, expressed as g/cm^2) and volumetric density (bone mass per volume area, expressed as g/cm^3) (1).

Several densitometric techniques can be used to provide *in vivo* measurements of BMD, such as DXA, quantitative computed tomography (QCT), and quantitative ultrasound (QUS) (11,12). Importantly, it has to be considered that clinical diagnosis of osteoporosis firstly relies on the occurrence of any of major fragility fracture (such as vertebral, hip or wrist fracture), despite the specific BMD value. In fact, it has been showed that only 39% of individuals with a vertebral fracture had a WHO diagnosis of osteoporosis by DXA at the spine, and only 25% by DXA of the total hip (13).

DXA

DXA is currently the most widely used quantitative bone imaging technique for BMD measurements both in clinical practice and in research studies (14). This quantitative technique provides areal BMD measurements expressed in in grams per square centimeter (g/cm^2), which is known

to represent a major determinant of bone strength and correlate to fracture risk (1).

The advantages of DXA are firstly related to the extremely low dose provided to patients, ranging from 1 to 6 μSv, which is considered negligible when compared to natural background radiation (2.4 mSv) (15,16). Secondly, DXA is able to measure BMD at those sites particularly relevant to osteoporotic fractures, such as lumbar spine and proximal femur, and measurements at these sites are optimal to predict fracture risk (17). The reproducibility of BMD measurements is very good, with a coefficient of variation (CoV) that ranges from 1% at lumbar spine to 2% at femoral neck (14,18,19). Lastly, DXA scans are widely available worldwide with very low scanning time (1–3 minutes).

Nevertheless, DXA areal BMD measurements has also some limitations, as they are influenced by changes in lumbar spine density due to osteoarthrosis or previous fracture which may be common in the elderly and usually increase BMD values (10,20). In addition, areal BMD measures is size-dependent thus leads to a BMD overestimation in large bones and a BMD underestimation in small bones, a limitation that can be problematic especially in children (21,22).

In order to obtaining a proper DXA scan the operator must pay attention to several aspects, such as patient demographic information, patient positioning and scan analysis. It has been showed that DXA quality is frequently affected by errors in acquisition, analysis and interpretation, and this may lead to inappropriate diagnosis and clinical decisions (20,23).

Diagnosing osteoporosis with DXA

BMD results obtained by DXA are usually expressed as T-score or Z-score. T-score represents the number of standard deviations by which BMD varies from the mean value expected in a young healthy subject (20–30 years of age), whereas Z-score is the number of standard deviations by which BMD varies from the mean value typical for a person with the same age and sex (1,24). According to the World Health Organization (WHO) definition of osteoporosis, the disease can be diagnosed when T-score ≤–2.5 of DXA at the lumbar spine, femoral neck or distal third of the radius (25,26). It is important to remind that this diagnostic cut-off does cannot be used when BMD is obtained with a technique different than DXA (14). When the T-score value is between –1.0 and –2.5 SDs, the patient

is diagnosed with osteopenia. Of note, the use of T-score with the traditional WHO densitometric classification is indicated only when reporting DXA of a postmenopausal woman or man age older than 50 years old, as suggested by the International Society for Clinical Densitometry (ISCD) Official Positions (27). When reporting a DXA of a premenopausal woman (from 20 years old to menopause) or the scan of a man aged between 20 and 50, Z-score is preferred to T-score. Furthermore, the traditional WHO operational classification of normal, osteopenia, and osteoporosis should be avoided. In fact, according to ISCD, a patient with a Z-score equal or lower than –2.0 is classified as having a BMD "below the expected range for age"; with a Z-score above –2.0 the patient is classified as having a BMD "within the expected range for age" (28).

Choosing the site to measure BMD with DXA

The so-called "central sites" are typically used to measure BMD with DXA. These sites are lumbar spine and proximal femur, with ISCD suggesting to evaluate both when performing the first examination (27). Forearm DXA is not routinely performed, but may be obtained when lumbar spine or hip cannot be measured (degenerative arthritis, vertebral fractures spinal surgery or total hip arthroplasty) (29). Also, due to its preferential involvement, DXA scan of the forearm is indicated in patients with hyperparathyroidism (30).

Lumbar spine DXA should include in the analysis the first four lumbar vertebrae (see *Figure 1*). Careful should be used when analyzing this site, as vertebrae may be commonly affected by structural changes and should be excluded from the analysis when the T-score difference with the adjacent vertebra is >1 (31).

Proximal femur scan requires proper position of the patient, which should be placed with the foot internally rotated for the femoral neck to be parallel to the table and the lesser trochanter to be hidden as much as possible (see *Figure 2*). Poor patient positioning is a potential cause of error (estimated 5% BMD variation) (14). Femoral neck is the preferred region for diagnosis, followed by "total femur" when the T-score is lower. Other proximal femur region should not be used for diagnosis due to intrinsic variability and lower reproducibility (27). In certain condition such as scoliosis, controversy exists about the possibility to scan both femurs (32).

When forearm DXA is necessary, the "33% radius" or "one-third radius" should be used as an alternative site for

diagnosis. Importantly, the non-dominant forearm should be scanned, due to the fact that dominant forearm usually presents with higher BMD values (33).

Additional tools of DXA

Despite BMD is the most widely used DXA parameter, this technique offers the possibility to obtain other supplementary quantitative measurements that can be used to improve the evaluation of patients with osteoporosis. These measurements showed the potential to improve fracture risk prediction, even though they are still not fully implemented in clinical practice such as the use of BMD.

Hip geometry obtained by two-dimensional DXA scans offers the possibility to evaluate several parameters, such as the proximal hip axis length (HAL), cross-sectional moment of inertia, the neck shaft angle and the cross-sectional area (see *Figure 3*). These measurements showed to correlate with three-dimensional parameters obtained with QCT (34); nevertheless, due to the weak association with fractures when controlling for BMD, a lack of consensus about the clinical use of hip geometry parameter (24,35). As a consequence, a recent position paper by the ISCD was issued in 2015 providing recommendations about hip geometry possible use for fracture risk prediction (36). In this review only the HAL was recommended for clinical use in women, due positive association between a longer HAL and hip fracture (36). More recently, this evidence was extended to male population, with a recent article showing a positive association between increased HAL in men and hip fracture risk (37).

Trabecular bone score (TBS) is a recently implemented tool that provides a grayscale textural analysis of lumbar spine DXA images, showing the potential to be a BMD-independent fracture risk predictor (18,38,39). TBS is able to measures the variations in gray-level texture between adjacent pixels from DXA raw data; *ex vivo* studies confirmed that TBS was strongly correlate to micro-CT parameters, such as bone volume, tissue volume or trabecular number (40,41). From a practical point of view, TBS values are easy to obtain as they are produced by a simple re-analysis of DXA BMD data, at the end of a normal scan (see *Figure 4*). Higher TBS values correlates with a better microarchitecture (with consequent better fracture resistance), whereas lower TBS values correlates with a weaker microarchitecture (42,43). As for hip geometry parameters, in 2015 ISCD produced official positions to recommend the use of TBS in certain clinical
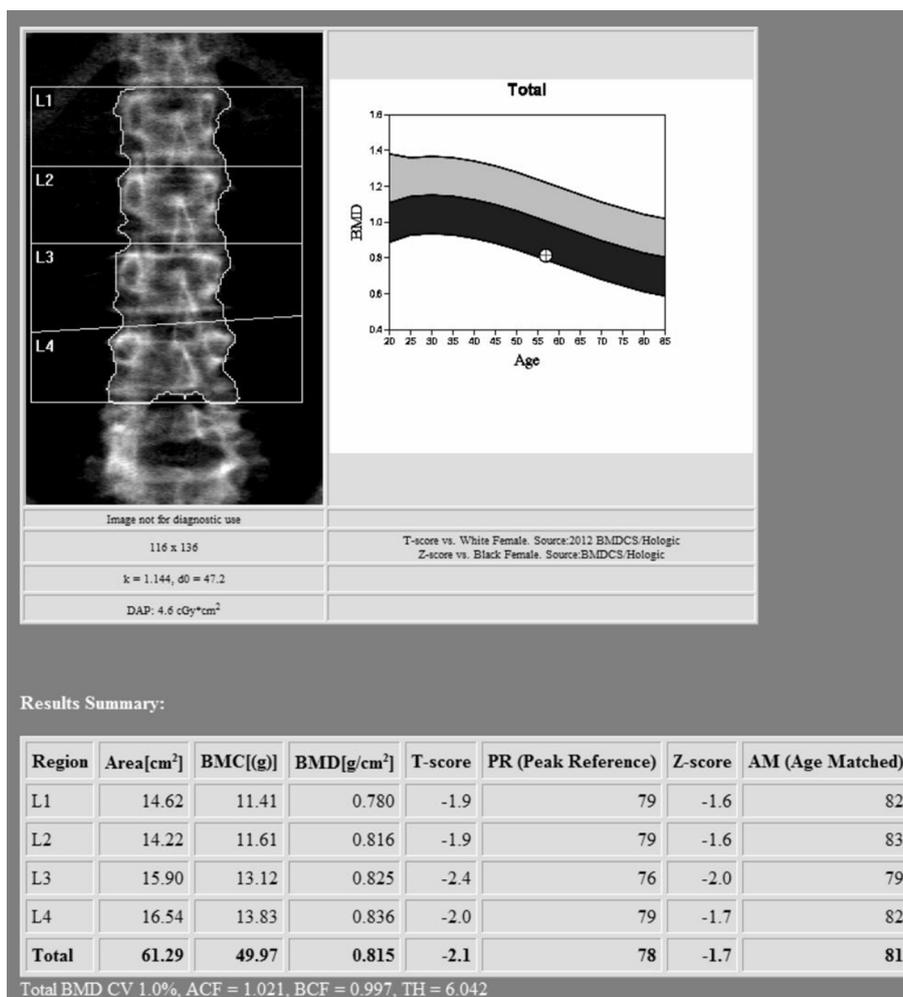
Region	Area[cm²]	BMC[(g)]	BMD[g/cm²]	T-score	PR (Peak Reference)	Z-score	AM (Age Matched)
L1	14.62	11.41	0.780	-1.9	79	-1.6	82
L2	14.22	11.61	0.816	-1.9	79	-1.6	83
L3	15.90	13.12	0.825	-2.4	76	-2.0	79
L4	16.54	13.83	0.836	-2.0	79	-1.7	82
Total	**61.29**	**49.97**	**0.815**	**-2.1**	**78**	**-1.7**	**81**

Total BMD CV 1.0%, ACF = 1.021, BCF = 0.997, TH = 6.042

Figure 1 Lumbar spine is one of the most commonly used site for DXA. Image shows proper positioning and analysis of the L1–L4 lumbar spine. Diagnosis should be made on the average L1–L4 value; at least two vertebrae must be used. DXA, dual-energy X-ray absorptiometry; BMC, body mineral content; BMD, bone mineral density.

situations (44). According to these recommendations, TBS can be used in association with BMD to evaluate fracture risk in postmenopausal women; the evidence for using TBS in men greater than 50 years of age was somehow lower (44). On the contrary, due to its lower reproducibility compared to BMD, the use of TBS alone is not recommended to evaluate osteoporotic treatment and determine treatment suggestions (44).

Quantitative vertebral morphometry can be performed with DXA by means of lateral images acquired with vertebral fracture assessment (VFA) scans. The purpose of quantitative vertebral morphometry is to obtain measurements of vertebral body heights in order to increase the reproducibility of qualitative readings, especially when evaluating atraumatic and asymptomatic vertebral deformities (in which the standard visual radiologic approach may lead to disagreements) (10). Currently, the semi-quantitative method of Genant is the most widely used for morphometry (45,46). VFA images (from the fourth thoracic vertebra to the fourth lumbar vertebra) can be obtained both with the patient in lateral or supine decubitus, the latter options being possible with newer scans equipped with a rotating "C-arm". VFA offers several advantages compared to standard radiography. First, it involves significantly lower amount of ionizing radiation, with a mean dose around 40 µSv (14,15). The second important advantage is that VFA does not suffer end-plate vertebral body distortion, as the exam is acquired with a
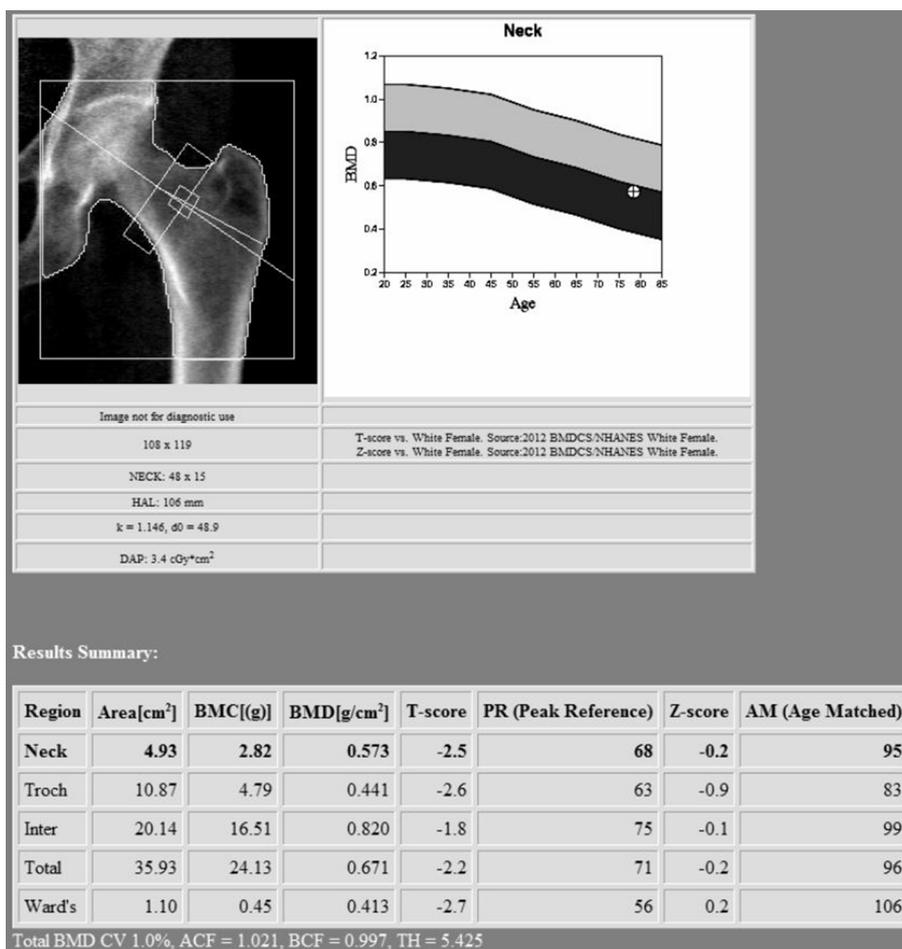
Figure 2 The image shows the proper way to position and analyse the proximal femur with DXA. The preferred region of interest (ROI) for diagnosis is femoral neck, but total hip ROI can be used if it presents lower values. DXA, dual-energy X-ray absorptiometry; BMC, body mineral content; BMD, bone mineral density.

divergent moving X-ray beam. Lastly, VFA images can be used for the evaluation and scoring of abdominal aortic calcification (47).

Non-DXA quantitative densitometric techniques

In addition to DXA, several other techniques allows for a quantitative skeletal assessment, with quantitative CT (QCT) and quantitative ultrasonography (QUS) being the two more commonly used in clinical practice (10). High-resolution peripheral CT and high-resolution MRI are able to provide a deeper evaluation of bone microarchitecture, but their clinical availability is still scarce and will not be discussed in this review. It is important to note that BMD and T-score values obtained with measurements other than

central DXA should not be used to diagnose patients with the WHO classification (27).

Compared to DXA, QCT is a cross-sectional technique that provides volumetric mineral density values, which are expressed in g/cm^3. As a consequence, QCT offers some advantages compared to DXA, such as the fact that volumetric BMD data are not size-dependent. In addition, CT is able to distinguish between cortical and trabecular components, providing separate BMD values (11). QCT can be applied to central sites (lumbar spine and hip) as well as to peripheral site (10). For hip and lumbar spine evaluation, QCT is acquired on the same CT scanner that is uses also for other clinical purposes. Peripheral site (usually tibia and radius) are acquired on dedicated scanners for peripheral anatomical sites (10). For central scanning,
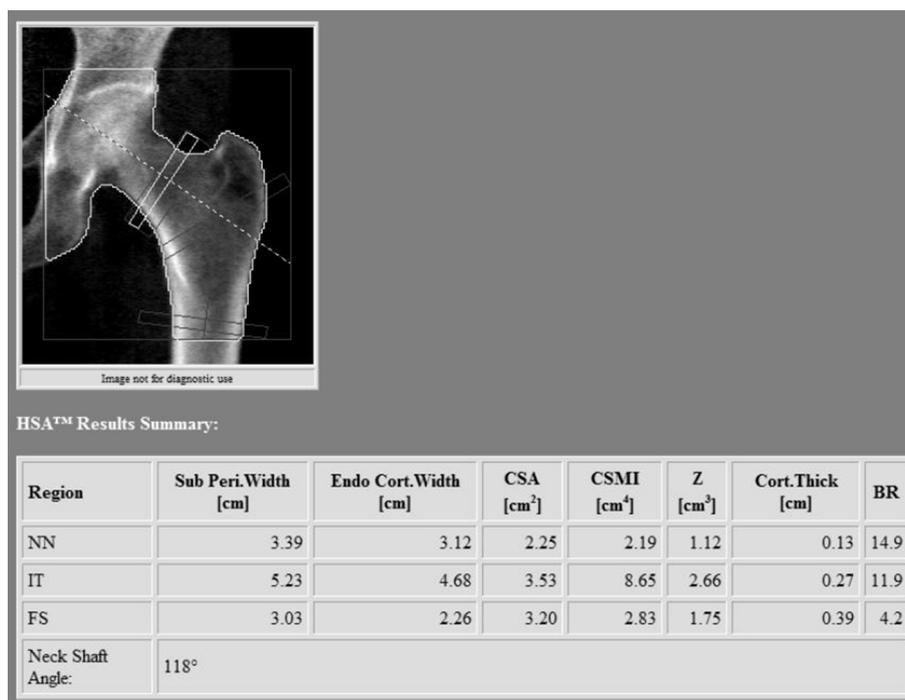
HSA™ Results Summary:

Region	Sub Peri.Width [cm]	Endo Cort.Width [cm]	CSA [cm^2]	CSMI [cm^4]	Z [cm^3]	Cort.Thick [cm]	BR
NN	3.39	3.12	2.25	2.19	1.12	0.13	14.9
IT	5.23	4.68	3.53	8.65	2.66	0.27	11.9
FS	3.03	2.26	3.20	2.83	1.75	0.39	4.2
Neck Shaft Angle:	118°						

Figure 3 Hip structural analysis (HSA) represents an additional tool of DXA. It provides information about several parameters of hip geometry obtained by two-dimensional DXA scans. DXA, dual-energy X-ray absorptiometry; CSA, cross-sectional area; CSMI, cross-sectional moment of inertia.
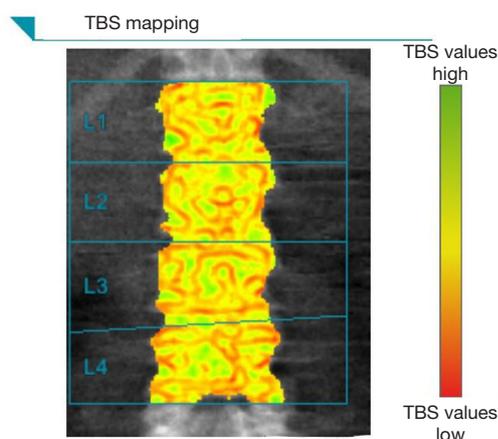

Figure 4 Trabecular bone score (TBS) is another additional and more recent tool provided by DXA. It offers an indirect analysis of bone microarchitecture, being a promising tool to use in adjunction with conventional BMD analysis. DXA, dual-energy X-ray absorptiometry; BMD, bone mineral density.

a phantom is required to calibrate the machine and obtain BMD values from standard Hounsfield unit (HU) CT values; nevertheless, recent developments allow for the use of clinical CT scan for the evaluation of BMD without the use of phantom calibration (48).

Vertebral QCT can measure BMD at thoracic and lumbar spine providing to patient a lower radiation dose compared to standard abdominal CT, but still higher than that of DXA. For hip QCT, which provide very useful information regarding trabecular and cortical bone at proximal femur, this dose is unfortunately even higher (14,15). Peripheral QCT scans performed at tibia and radius provide very low radiation dose and allow for the evaluation of cortical and trabecular bone content, as well as BMD values. Additionally, biomechanical and geometrical parameters can be obtained, leading to a comprehensive evaluation of bone microarchitecture and strength (48).

Imaging of sarcopenia

The assessment of body composition (BC) for suspected sarcopenia can be done with both non-imaging and imaging techniques. Among the non-imaging tools, bioelectrical impedance analysis (BIA) is the most commonly used,

being a low-cost and, non-invasive and widely spread technique. The working principle behind BIA relies on the application of an electric current across the body, which allows for the estimation of total muscle mass on the basis of current conduction (49). This is possible thanks to the fact that muscle represents the human body tissue with the largest percentage of water. With BIA is possible to obtain information about the fat-free mass and total body water (49). Nevertheless, measurements may be inaccurate in subjects with fluid and electrolyte abnormalities, such as excessive/low hydration or in the presence of soft-tissue edema. Thus, non-imaging techniques are mostly used as screening techniques, with imaging playing an increasing role in the diagnosis of sarcopenia (50). The most common BC imaging-techniques are DXA, CT and magnetic resonance imaging (MRI).

Evaluating BC with DXA

DXA currently represent the most commonly used technique for the estimation of BC at molecular level. As for BMD measurements, the principle behind DXA measurement is the transmission across the human body of an X-ray source at two different energy levels. This allows, after different degrees of X-ray attenuation by human tissue, to estimate fat mass (FM), lean mass (LM) and body mineral content (BMC), thus providing a three-compartment model of BC (51,52). Importantly, it has to be pointed out that DXA is not the gold standard technique for assessing BC, as it does not provide a direct measurement of these three components (53). In fact, image areas displaying bone allows DXA only for distinguish between bone and the remaining soft tissue (LM together with FM), but it is not possible to directly quantify the exact amount of LM and FM alone (54). To overcome this limitation, the software estimates the amount of LM and FM by calculating it in the adjacent areas, assuming that soft tissue BC is similar to bone-free tissues. Despite this, DXA measurements of BC offers very good values of accuracy and precision and have been have been validated in several clinical settings, showing a very good correlation with BC measurements obtained with other techniques such as CT and MRI (52,55). In addition to its clinical scope, the use of BC DXA in the research setting is increasing, being introduced in the evaluation of several conditions such as athletes physical performance, paediatric diseases, epidemiologic studies (56).

Diagnosing sarcopenia with DXA

With the increasing use of DXA and other BC quantitative techniques, the diagnostic definition of sarcopenia has necessarily evolved. The current description of sarcopenia includes impairment in both muscle quantity and muscle quality (57). Quantitative assessment of muscle mass can be done by DXA, but this evaluation should always be accompanied by qualitative assessment by means of physical performance evaluation (58). Several BC parameters can be obtained with DXA: appendicular lean mass (ALM), representing the sum of lean mass at upper and lower limbs; appendicular lean mass index (ALMI = ALM/height^2); android/gynoid ratio; fat mass index (FMI = fat mass/height^2). *Figure 5* shows an example of DXA BC assessment. ALMI is currently the most used measurement for assessing sarcopenia (58). According to ISCD, a definition of "low lean mass" could be done using ALMI with proper values of Z-scores obtained from a young adult, gender, and race matched population. Currently, a value of ALMI less than 2 Z-score is the most often used parameter to diagnose sarcopenia with BC DXA, as this cut-off is strongly associated with functional disabilities in the elderly (58-60). Some absolute thresholds have been proposed; the most commonly reported diagnostic values for sarcopenia are shown in *Table 1*. Nevertheless, these values still await for further confirmation from larger epidemiological studies (58).

MRI

MRI, together with CT, are currently considered the reference standard for BC evaluation, as both techniques produce cross-sectional images allowing for segmental and total measures of fat and lean mass (67,68).

MRI is capable to produce high-resolution images with great depiction of the different soft tissue components (muscle, fat mass, water) based on the different molecular properties of anatomical compartments. For what concerns the qualitative assessment, MRI is capable to depict at the same time qualitative abnormalities such as muscle disruption, edema or the presence of intramuscular adipose tissue/fibrosis (50) (see *Figure 6*). On the other side, MRI offers the possibility to assess muscle composition by using several quantitative techniques. Among these, Dixon MIR sequences offer the possibility for water-fat separated MRI evaluation, allowing for precise measurements of muscle
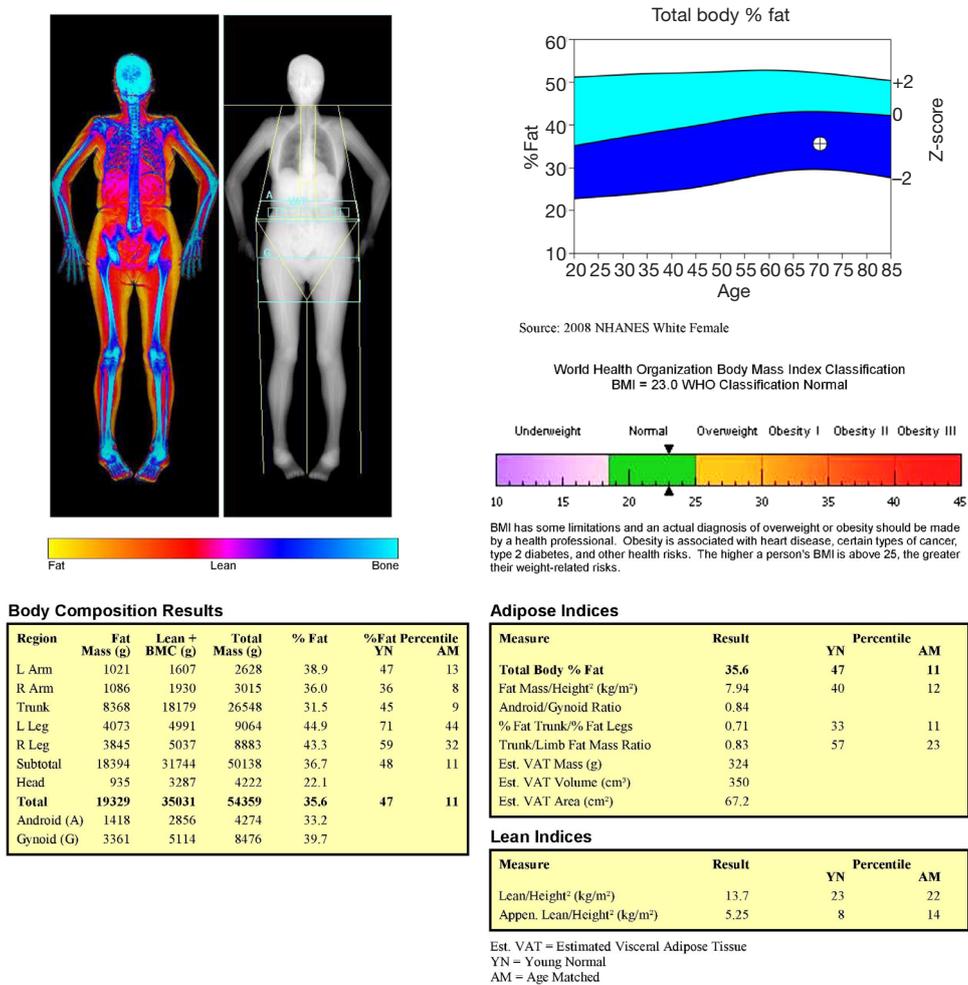
Body Composition Results

Region	Fat Mass (g)	Lean + BMC (g)	Total Mass (g)	% Fat	%Fat Percentile YN	%Fat Percentile AM
L Arm	1021	1607	2628	38.9	47	13
R Arm	1086	1930	3015	36.0	36	8
Trunk	8368	18179	26548	31.5	45	9
L Leg	4073	4991	9064	44.9	71	44
R Leg	3845	5037	8883	43.3	59	32
Subtotal	18394	31744	50138	36.7	48	11
Head	935	3287	4222	22.1		
Total	19329	35031	54359	35.6	47	11
Android (A)	1418	2856	4274	33.2		
Gynoid (G)	3361	5114	8476	39.7		

Adipose Indices

Measure	Result	Percentile YN	Percentile AM
Total Body % Fat	35.6	47	11
Fat Mass/Height^2 (kg/m^2)	7.94	40	12
Android/Gynoid Ratio	0.84		
% Fat Trunk/% Fat Legs	0.71	33	11
Trunk/Limb Fat Mass Ratio	0.83	57	23
Est. VAT Mass (g)	324		
Est. VAT Volume (cm^3)	350		
Est. VAT Area (cm^2)	67.2		

Lean Indices

Measure	Result	Percentile YN	Percentile AM
Lean/Height^2 (kg/m^2)	13.7	23	22
Appen. Lean/Height^2 (kg/m^2)	5.25	8	14

Est. VAT = Estimated Visceral Adipose Tissue
YN = Young Normal
AM = Age Matched

Figure 5 Body composition results showing a graphical body scan with different colours, according to the percentage of fat mass, lean mass and bone (depicted in yellow, red and blue, respectively). Body mass index (BMI) is represented, according to World Health Organization classification. Adipose and lean indices are reported as well. Appen. lean/height² (kg/m²) represents the appendicular lean mass index (ALMI), commonly used for diagnosing sarcopenia. BMC, body mineral content.

Table 1 Main ALMI (appendicular lean mass index) cut-offs values proposed for the diagnosis of sarcopenia with BC DXA

Reference	Year	ALMI cut-offs (kg/m²) Women	ALMI cut-offs (kg/m²) Men
Coin *et al.* (61)	2013	<5.47	<7.59
Morley *et al.* (62)	2011	<5.45	<7.26
Cruz-Jentoft *et al.* (4)	2010	<5.67	<7.25
Muscaritoli *et al.* (63)	2010	<5.67	<7.25
Delmonico *et al.* (64)	2007	<5.67	<7.25
Newman *et al.* (65)	2003	<5.67	<7.25
Baumgartner *et al.* (66)	1998	<5.45	<7.26

BC, body composition; DXA, dual-energy X-ray absorptiometry.

qims.amegroups.com   *Quant Imaging Med Surg* 2018;8(1):86-99

94

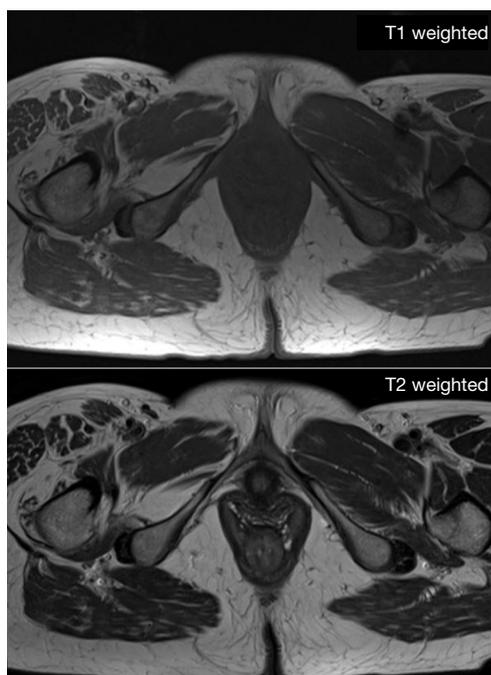**Messina et al. Imaging of osteoporosis and sarcopenia**

Figure 6 Magnetic resonance imaging (MRI) of a 53 years old female with right lumbosacral radiculoplexus neuropathy. Both T1- and T2-weighted images show severe fatty infiltration of pelvic and thigh muscles on the right side. The left side is normal.

volume and the degree of fat infiltration (see *Figure 7*) (69,70). Automatic segmentation was also proposed for evaluating total body and regional muscle volume by means of Dixon MRI sequences (71). MRI with diffusion tensor imaging (DTI) is able to measure anisotropy in water diffusion, thus providing a measure of muscle fibers arrangement (72). Therefore, DTI can be used to evaluate muscle microstructure and demonstrate fatty infiltration (69). The use of MRI spectroscopy is a further possibility offered to precisely quantify the percentage of intracellular fat, which may be increased in several conditions such as cancer or insulin resistance (50,73). As a further advantage, the use of MRI involves no exposure to ionizing radiation, in contrast with CT and DXA. For all these reasons, MRI is the most advanced and reliable imaging techniques for studying BC. Nevertheless, drawbacks of MRI are the high cost of examinations, its complexity as well as its limited availability; consequently, despite its superiority, the use of MRI for BC remains limited in clinical practice, being mainly relegated to research use (74,75).

CT

As previously stated, CT is another cross sectional imaging method that is able to discriminate between different tissue based on their different X-ray attenuation, thus providing information on muscle quantity and composition (10,76). Normal attenuation values for muscle density are variable ranging from 40 to 100 HU; with fatty infiltration, muscle shows variable size areas of decreased HU values (between −200 and −35 HU) (77). Conventionally, HU value of water is 0 and HU value of air is −1,000.

Muscular fatty infiltration is most commonly associated with aging, but it can be seen with disuse or pathological conditions. Apart from qualitative evaluation, the amount of intramuscular adipose tissue can be quantified with post-processing analysis (69). After excluding visceral organs, muscle segmentation can be done using HU density thresholds: images are selected at a specific plane, segmenting all muscle with software analysis set to include tissue from −20 to 150 HU (50,78). This evaluation is commonly performed at L4 level to measure cross-sectional area of psoas muscle, as well as to measure paraspinal musculature usually at T12 level. High quality reconstruction images can be obtained with CT and may be helpful in increasing segmentation accuracy.

The radiation exposure of CT represents a non-negligible limitation of this technique and limits its clinical application. Apart for research setting, CT quantitative evaluation has been proposed as an additional tool to diagnose sarcopenia in patients already undergoing CT examinations for other reasons, such as major surgery or oncologic diseases (50).

Conclusions

Osteoporosis and sarcopenia are two chronic diseases representing a major clinical problem with increasing prevalence in the elderly. The combination of these diseases has non-negligible impact on quality life and survival due to the possible occurrence of falls, fractures and frailty. It is therefore mandatory to properly diagnose such entities in order to prevent their clinical onset. DXA is widely recognized as the reference standard for the diagnosis and management of osteoporosis, and will probably remain so for the next future. In addition, DXA offers the possibility to assess BC: it is a low-cost technique, widely available and provides accurate and precise values compared to
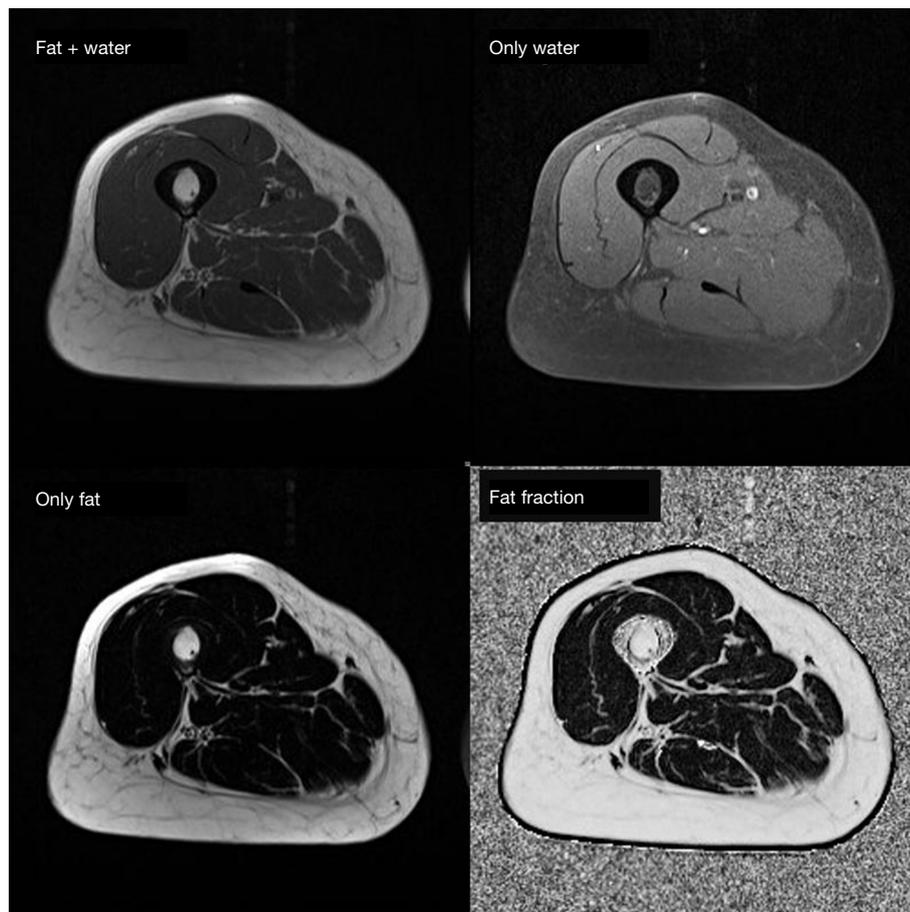
Figure 7 Example of the use of Dixon MRI sequences to evaluate separately water and fat components in a thigh. The sequence provides four images: both fat and water components, water and fat only, and fat fraction that can be used for quantification purposes.

CT and MRI (currently considered the gold standard). For this reason, DXA is currently the most frequently used technique to image sarcopenia, not only for research application but also for clinical purposes.

Footnote

Conflicts of Interest: The authors have no conflicts of interest to declare.

References

1. Kanis JA, McCloskey EV, Johansson H, Cooper C, Rizzoli R, Reginster JY. European guidance for the diagnosis and management of osteoporosis in postmenopausal women. Osteoporos Int 2013;24:23-57.

2. Beaudart C, Dawson A, Shaw SC, Harvey NC, Kanis JA, Binkley N, Reginster JY, Chapurlat R, Chan DC, Bruyère O, Rizzoli R, Cooper C, Dennison EM, IOF-ESCEO Sarcopenia Working Group. Nutrition and physical activity in the prevention and treatment of sarcopenia: systematic review. Osteoporos Int 2017;28:1817-33.

3. Consensus development conference: diagnosis, prophylaxis, and treatment of osteoporosis. Am J Med 1993;94:646-50.

4. Cruz-Jentoft AJ, Baeyens JP, Bauer JM, Boirie Y, Cederholm T, Landi F, Martin FC, Michel JP, Rolland Y, Schneider SM, Topinkova E, Vandewoude M, Zamboni M, European Working Group on Sarcopenia in Older People. Sarcopenia: European consensus on definition and

diagnosis: Report of the European Working Group on Sarcopenia in Older People. Age Ageing 2010;39:412-23.

5. Hirschfeld HP, Kinsella R, Duque G. Osteosarcopenia: where bone, muscle, and fat collide. Osteoporos Int 2017;28:2781-90.

6. Cooper C, Atkinson EJ, Jacobsen SJ, O'Fallon WM, Melton LJ. Population-based study of survival after osteoporotic fractures. Am J Epidemiol 1993;137:1001-5.

7. Miyakoshi N, Hongo M, Mizutani Y, Shimada Y. Prevalence of sarcopenia in Japanese women with osteopenia and osteoporosis. J Bone Miner Metab 2013;31:556-61.

8. Di Monaco M, Vallero F, Di Monaco R, Tappero R. Prevalence of sarcopenia and its association with osteoporosis in 313 older women following a hip fracture. Arch Gerontol Geriatr 2011;52:71-4.

9. Lima RM, Bezerra LM, Rabelo HT, Silva MA, Silva AJ, Bottaro M, de Oliveira RJ. Fat-free mass, strength, and sarcopenia are related to bone mineral density in older women. J Clin Densitom 2009;12:35-41.

10. Guglielmi G, Muscarella S, Bazzocchi A. Integrated imaging approach to osteoporosis: state-of-the-art review and update. Radiographics 2011;31:1343-64.

11. Engelke K, Glüer CC. Quality and performance measures in bone densitometry. Osteoporos Int 2006;17:1283-92.

12. Oei L, Koromani F, Rivadeneira F, Zillikens MC, Oei EH. Quantitative imaging methods in osteoporosis. Quant Imaging Med Surg 2016;6:680-98.

13. Stone KL, Seeley DG, Lui LY, Cauley JA, Ensrud K, Browner WS, Nevitt MC, Cummings SR, Osteoporotic Fractures Research Group. BMD at multiple sites and risk of fracture of multiple types: long-term results from the Study of Osteoporotic Fractures. J Bone Miner Res 2003;18:1947-54.

14. Adams JE. Advances in bone imaging for osteoporosis. Nat Rev Endocrinol 2013;9:28-42.

15. Damilakis J, Adams JE, Guglielmi G, Link TM. Radiation exposure in X-ray-based imaging techniques used in osteoporosis. Eur Radiol 2010;20:2707-14.

16. Bandirali M, Lanza E, Messina C, Sconfienza LM, Brambilla R, Maurizio R, Marchelli D, Piodi LP, Di Leo G, Ulivieri FM, Sardanelli F. Dose absorption in lumbar and femoral dual energy X-ray absorptiometry examinations using three different scan modalities: an anthropomorphic phantom study. J Clin Densitom 2013;16:279-82.

17. Marshall D, Johnell O, Wedel H. Meta-analysis of how well measures of bone mineral density predict occurrence of osteoporotic fractures. BMJ 1996;312:1254-9.

18. Bandirali M, Poloni A, Sconfienza LM, Messina C, Papini GD, Petrini M, Ulivieri FM, Di Leo G, Sardanelli F. Short-term precision assessment of trabecular bone score and bone mineral density using dual-energy X-ray absorptiometry with different scan modes: an in vivo study. Eur Radiol 2015;25:2194-8.

19. Delnevo A, Bandirali M, Di Leo G, Messina C, Sconfienza LM, Aliprandi A, Ulivieri FM, Sardanelli F. Differences among array, fast array, and high-definition scan modes in bone mineral density measurement at dual-energy x-ray absorptiometry on a phantom. Clin Radiol 2013;68:616-9.

20. Messina C, Bandirali M, Sconfienza LM, D'Alonzo NK, Di Leo G, Papini GDE, Ulivieri FM, Sardanelli F. Prevalence and type of errors in dual-energy x-ray absorptiometry. Eur Radiol 2015;25:1504-11.

21. Bachrach LK. Assessing bone health in children: who to test and what does it mean? Pediatr Endocrinol Rev 2005;2 Suppl 3:332-6.

22. Wasserman H, Gordon CM. Bone Mineralization and Fracture Risk Assessment in the Pediatric Population. J Clin Densitom 2017;20:389-96.

23. Morgan SL, Prater GL. Quality in dual-energy X-ray absorptiometry scans. Bone 2017;104:13-28.

24. Jain RK, Vokes T. Dual-energy X-ray Absorptiometry. J Clin Densitom 2017;20:291-303.

25. WHO Study Group. Assessment of fracture risk and its application to screening for postmenopausal osteoporosis. WHO, Geneva, Switzerland (WHO Technical Report Series 843, 1994).

26. Kanis JA, on behalf of the WHO Scientific Group (2008). Assessment of osteoporosis at the primary health-care level. Technical Report. WHO Collaborating Centre, University of Sheffield, UK.

27. Lewiecki EM, Gordon CM, Baim S, Leonard MB, Bishop NJ, Bianchi ML, Kalkwarf HJ, Langman CB, Plotkin H, Rauch F, Zemel BS, Binkley N, Bilezikian JP, Kendler DL, Hans DB, Silverman S. International Society for Clinical Densitometry 2007 Adult and Pediatric Official Positions. Bone 2008;43:1115-21.

28. International Society for Clinical Densitometry (ISCD) Skeletal Health [Internet]. 2015 [cited 2017 Oct 28]. Available online: http://www.iscd.org/official-positions/2015-iscd-official-positions-adult/

29. Messina C, Sconfienza L, Bandirali M, Guglielmi G, Ulivieri F. Adult Dual-Energy X-ray Absorptiometry in Clinical Practice: How I Report it. Semin Musculoskelet Radiol 2016;20:246-53.

30. Bilezikian JP, Brandi ML, Eastell R, Silverberg SJ,

Udelsman R, Marcocci C, Potts JT. Guidelines for the management of asymptomatic primary hyperparathyroidism: summary statement from the Fourth International Workshop. J Clin Endocrinol Metab 2014;99:3561-9.

31. Hamdy RC, Petak SM, Lenchik L. Which central dual X-ray absorptiometry skeletal sites and regions of interest should be used to determine the diagnosis of osteoporosis? J Clin Densitom 2002;5 Suppl:S11-8.

32. Bandirali M, Messina C, Di Leo G, Sconfienza LM, Aliprandi A, Ulivieri FM, Sardanelli F. Bone mineral density differences between femurs of scoliotic patients undergoing dual-energy X-ray absorptiometry. Clin Radiol 2013;68:e511-5.

33. Walters J, Koo WW, Bush A, Hammami M. Effect of hand dominance on bone mass measurement in sedentary individuals. J Clin Densitom 1998;1:359-67.

34. Prevrhal S, Shepherd JA, Faulkner KG, Gaither KW, Black DM, Lang TF. Comparison of DXA hip structural analysis with volumetric QCT. J Clin Densitom 2008;11:232-6.

35. Kaptoge S, Beck TJ, Reeve J, Stone KL, Hillier TA, Cauley JA, Cummings SR. Prediction of incident hip fracture risk by femur geometry variables measured by hip structural analysis in the study of osteoporotic fractures. J Bone Miner Res 2008;23:1892-904.

36. Broy SB, Cauley JA, Lewiecki ME, Schousboe JT, Shepherd JA, Leslie WD. Fracture Risk Prediction by Non-BMD DXA Measures: the 2015 ISCD Official Positions Part 1: Hip Geometry. J Clin Densitom 2015;18:287-308.

37. Leslie WD, Lix LM, Morin SN, Johansson H, Odén A, McCloskey EV, Kanis JA. Adjusting Hip Fracture Probability in Men and Women Using Hip Axis Length: the Manitoba Bone Density Database. J Clin Densitom 2016;19:326-31.

38. Shevroja E, Lamy O, Kohlmeier L, Koromani F, Rivadeneira F, Hans D. Use of Trabecular Bone Score (TBS) as a Complementary Approach to Dual-energy X-ray Absorptiometry (DXA) for Fracture Risk Assessment in Clinical Practice. J Clin Densitom 2017;20:334-45.

39. Bonaccorsi G, Fila E, Messina C, Maietti E, Ulivieri FM, Caudarella R, Greco P, Guglielmi G. Comparison of trabecular bone score and hip structural analysis with FRAX(®) in postmenopausal women with type 2 diabetes mellitus. Aging Clin Exp Res 2017;29:951-7.

40. Roux JP, Wegrzyn J, Boutroy S, Bouxsein ML, Hans D, Chapurlat R. The predictive value of trabecular bone score (TBS) on whole lumbar vertebrae mechanics: an ex vivo study. Osteoporos Int 2013;24:2455-60.

41. Winzenrieth R, Michelet F, Hans D. Three-dimensional (3D) microarchitecture correlations with 2D projection image gray-level variations assessed by trabecular bone score using high-resolution computed tomographic acquisitions: effects of resolution and noise. J Clin Densitom 2013;16:287-96.

42. Silva BC, Leslie WD. Trabecular Bone Score: A New DXA-Derived Measurement for Fracture Risk Assessment. Endocrinol Metab Clin North Am 2017;46:153-80.

43. Bandirali M, Di Leo G, Messina C, Pastor Lopez MJ, Mai A, Ulivieri FM, Sardanelli F. Reproducibility of trabecular bone score with different scan modes using dual-energy X-ray absorptiometry: a phantom study. Skeletal Radiol 2015;44:573-6.

44. Silva BC, Broy SB, Boutroy S, Schousboe JT, Shepherd JA, Leslie WD. Fracture Risk Prediction by Non-BMD DXA Measures: the 2015 ISCD Official Positions Part 2: Trabecular Bone Score. J Clin Densitom 2015;18:309-30.

45. Guglielmi G, Diacinti D, van Kuijk C, Aparisi F, Krestan C, Adams JE, Link TM. Vertebral morphometry: current methods and recent advances. Eur Radiol 2008;18:1484-96.

46. Genant HK, Wu CY, van Kuijk C, Nevitt MC. Vertebral fracture assessment using a semiquantitative technique. J Bone Miner Res 1993;8:1137-48.

47. Schousboe JT, Taylor BC, Kiel DP, Ensrud KE, Wilson KE, McCloskey EV. Abdominal aortic calcification detected on lateral spine images from a bone densitometer predicts incident myocardial infarction or stroke in older women. J Bone Miner Res 2008;23:409-16.

48. Engelke K. Quantitative Computed Tomography-Current Status and New Developments. J Clin Densitom 2017;20:309-21.

49. Kyle UG, Bosaeus I, De Lorenzo AD, Deurenberg P, Elia M, Gómez JM, Heitmann BL, Kent-Smith L, Melchior JC, Pirlich M, Scharfetter H, Schols AM, Pichard C, Composition of the ESPEN Working Group. Bioelectrical impedance analysis--part I: review of principles and methods. Clin Nutr 2004;23:1226-43.

50. Boutin RD, Yao L, Canter RJ, Lenchik L. Sarcopenia: Current Concepts and Imaging Implications. AJR Am J Roentgenol 2015;205:W255-66.

51. Guglielmi G, Ponti F, Agostini M, Amadori M, Battista G, Bazzocchi A. The role of DXA in sarcopenia. Aging Clin Exp Res 2016;28:1047-60.

52. Messina C, Monaco CG, Ulivieri FM, Sardanelli F, Sconfienza LM. Dual-energy X-ray absorptiometry body composition in patients with secondary osteoporosis. Eur J

98

Messina et al. Imaging of osteoporosis and sarcopenia

Radiol 2016;85:1493-8.

53. Erlandson MC, Lorbergs AL, Mathur S, Cheung AM. Muscle analysis using pQCT, DXA and MRI. Eur J Radiol 2016;85:1505-11.

54. Toombs RJ, Ducher G, Shepherd JA, De Souza MJ. The impact of recent technological advances on the trueness and precision of DXA to assess body composition. Obesity (Silver Spring) 2012;20:30-9.

55. Kullberg J, Brandberg J, Angelhed JE, Frimmel H, Bergelin E, Strid L, Ahlström H, Johansson L, Lönn L. Whole-body adipose tissue analysis: comparison of MRI, CT and dual energy X-ray absorptiometry. Br J Radiol 2009;82:123-30.

56. Krueger D, Binkley N. Total Body DXA: On the Cusp of Clinical Care. J Clin Densitom 2012;15:387-8.

57. Cederholm TE, Bauer JM, Boirie Y, Schneider SM, Sieber CC, Rolland Y. Toward a definition of sarcopenia. Clin Geriatr Med 2011;27:341-53.

58. Petak S, Barbu CG, Yu EW, Fielding R, Mulligan K, Sabowitz B, Wu CH, Shepherd JA. The Official Positions of the International Society for Clinical Densitometry: body composition analysis reporting. J Clin Densitom 2013;16:508-19.

59. Kyle UG, Genton L, Hans D, Karsegard VL, Michel JP, Slosman DO, Pichard C. Total body mass, fat mass, fat-free mass, and skeletal muscle in older people: cross-sectional differences in 60-year-old persons. J Am Geriatr Soc 2001;49:1633-40.

60. Bouchard DR, Dionne IJ, Brochu M. Sarcopenic/obesity and physical capacity in older men and women: data from the Nutrition as a Determinant of Successful Aging (NuAge)-the Quebec longitudinal Study. Obesity (Silver Spring) 2009;17:2082-8.

61. Coin A, Sarti S, Ruggiero E, Giannini S, Pedrazzoni M, Minisola S, Rossini M, Del Puente A, Inelmen EM, Manzato E, Sergi G. Prevalence of Sarcopenia Based on Different Diagnostic Criteria Using DEXA and Appendicular Skeletal Muscle Mass Reference Values in an Italian Population Aged 20 to 80. J Am Med Dir Assoc 2013;14:507-12.

62. Morley JE, Abbatecola AM, Argiles JM, Baracos V, Bauer J, Bhasin S, Cederholm T, Coats AJ, Cummings SR, Evans WJ, Fearon K, Ferrucci L, Fielding RA, Guralnik JM, Harris TB, Inui A, Kalantar-Zadeh K, Kirwan BA, Mantovani G, Muscaritoli M, Newman AB, Rossi-Fanelli F, Rosano GM, Roubenoff R, Schambelan M, Sokol GH, Storer TW, Vellas B, von Haehling S, Yeh SS, Anker SD; Society on Sarcopenia, Cachexia and Wasting Disorders Trialist Workshop. Sarcopenia with limited mobility: an international consensus. J Am Med Dir Assoc 2011;12:403-9.

63. Muscaritoli M, Anker SD, Argilés J, Aversa Z, Bauer JM, Biolo G, Boirie Y, Bosaeus I, Cederholm T, Costelli P, Fearon KC, Laviano A, Maggio M, Rossi Fanelli F, Schneider SM, Schols A, Sieber CC. Consensus definition of sarcopenia, cachexia and pre-cachexia: joint document elaborated by Special Interest Groups (SIG) "cachexia-anorexia in chronic wasting diseases" and "nutrition in geriatrics". Clin Nutr 2010;29:154-9.

64. Delmonico MJ, Harris TB, Lee JS, Visser M, Nevitt M, Kritchevsky SB, Tylavsky FA, Newman AB; Health, Aging and Body Composition Study. Alternative definitions of sarcopenia, lower extremity performance, and functional impairment with aging in older men and women. J Am Geriatr Soc 2007;55:769-74.

65. Newman AB, Kupelian V, Visser M, Simonsick E, Goodpaster B, Nevitt M, Kritchevsky SB, Tylavsky FA, Rubin SM, Harris TB; Health ABC Study Investigators. Sarcopenia: alternative definitions and associations with lower extremity function. J Am Geriatr Soc 2003;51:1602-9.

66. Baumgartner RN, Koehler KM, Gallagher D, Romero L, Heymsfield SB, Ross RR, Garry PJ, Lindeman RD. Epidemiology of sarcopenia among the elderly in New Mexico. Am J Epidemiol 1998;147:755-63.

67. Andreoli A, Scalzo G, Masala S, Tarantino U, Guglielmi G. Body composition assessment by dual-energy X-ray absorptiometry (DXA). Radiol Med 2009;114:286-300.

68. Levine JA, Abboud L, Barry M, Reed JE, Sheedy PF, Jensen MD. Measuring leg muscle and fat mass in humans: comparison of CT and dual-energy X-ray absorptiometry. J Appl Physiol 2000;88:452-6.

69. Heymsfield SB, Gonzalez MC, Lu J, Jia G, Zheng J. Skeletal muscle mass and quality: evolution of modern measurement concepts in the context of sarcopenia. Proc Nutr Soc 2015;74:355-66.

70. Dixon WT. Simple proton spectroscopic imaging. Radiology 1984;153:189-94.

71. Karlsson A, Rosander J, Romu T, Tallberg J, Grönqvist A, Borga M, Dahlqvist Leinhard O. Automatic and quantitative assessment of regional muscle volume by multi-atlas segmentation using whole-body water-fat MRI. J Magn Reson Imaging 2015;41:1558-69.

72. Kim HK, Lindquist DM, Serai SD, Mariappan YK, Wang LL, Merrow AC, McGee KP, Ehman RL, Laor T. Magnetic resonance imaging of pediatric muscular disorders: recent advances and clinical applications. Radiol

Clin North Am 2013;51:721-42.

73. Ermetici F, Briganti S, Delnevo A, Cannaò P, Leo GD, Benedini S, Terruzzi I, Sardanelli F, Luzi L. Bone marrow fat contributes to insulin sensitivity and adiponectin secretion in premenopausal women. Endocrine 2018;59:410-8.

74. Rubbieri G, Mossello E, Di Bari M. Techniques for the diagnosis of sarcopenia. Clin Cases Miner Bone Metab 2014;11:181-4.

75. Sergi G, Trevisan C, Veronese N, Lucato P, Manzato E. Imaging of sarcopenia. Eur J Radiol 2016;85:1519-24.

76. Goodpaster BH, Carlson CL, Visser M, Kelley DE, Scherzinger A, Harris TB, Stamm E, Newman AB.

Attenuation of skeletal muscle and strength in the elderly: The Health ABC Study. J Appl Physiol 2001;90:2157-65.

77. Sjöström L, Kvist H, Cederblad A, Tylén U. Determination of total adipose tissue and body fat in women by computed tomography, 40K, and tritium. Am J Physiol 1986;250:E736-45.

78. Martin L, Birdsell L, Macdonald N, Reiman T, Clandinin MT, McCargar LJ, Murphy R, Ghosh S, Sawyer MB, Baracos VE. Cancer cachexia in the age of obesity: skeletal muscle depletion is a powerful prognostic factor, independent of body mass index. J Clin Oncol 2013;31:1539-47.